Collective atomic dynamics in liquid $Rb_{95}Sb_5$



1997 J. Phys.: Condens. Matter 9 11035

(http://iopscience.iop.org/0953-8984/9/50/009)

J. Phys.: Condens. Matter **9** (1997) 11035–11043. Printed in the UK PII: S0953-8984(97)85526-9

# Collective atomic dynamics in liquid $Rb_{95}Sb_5$

G Pratesi† and J-B Suck‡

† Institut Laue-Langevin, BP 156, F-38042 Grenoble Cedex 9, France

‡ Institute of Physics, Material Research and Liquids, TU Chemnitz, D-09107, Chemnitz, Germany

Received 18 June 1997, in final form 6 October 1997

**Abstract.** The collective atomic dynamics of liquid $Rb_{95}Sb_5$ has been investigated at 920 K using cold neutron inelastic scattering techniques. The isothermal and the adiabatic dispersion curves together with the damping function of the viscosity have been obtained from a fit of Lovesey's model to the measured total dynamic structure factor $S(Q, \omega)$. The comparison of the total structure factor $S(Q)$ and the dispersion obtained from the maxima $\omega_m$ of the current–current correlation function for liquid $Rb_{95}Sb_5$ with the same functions obtained before for pure rubidium shows a small shortening and strengthening of the bonds in liquid $Rb_{95}Sb_5$ with respect to the bonds in pure liquid Rb, even though the character of the alloy is still metallic in general at this small Sb concentration.

## 1. Introduction

In recent years considerable progress has been made in the research of pure liquid metals, in particular their atomic dynamics, and even some properties very difficult to access have been studied, such as for example, the metal–nonmetal transition which occurs near the liquid–vapour critical point in pure alkali metals like Rb and Cs [1, 2].

Less well studied than pure liquid metals are liquid alloys of which several, composed of pure liquid metals, exhibit strong deviations from simple metallic behaviour in their electronic and thermodynamic properties in certain ranges of concentrations and temperatures. Near special stoichiometric compositions they may lose their metallic character, showing a transition from metallic to an ionic or a covalent character in their interatomic bonding [3].

Some experiments have been done varying the relative concentration of the components to study the electric and the thermodynamic properties [4, 5] or the static structure factor [6] in order to observe the metal–nonmetal transition. The conductivity and the thermodynamic properties of the alkali metal–antimony alloys are one of the best studied examples of this kind [7].

Although measurements of the conductivity and of thermodynamic properties give some hints on the character of the bonds, further information on the type of bonding in the alloys can be obtained by the investigation of the atomic dynamics by means of neutron inelastic scattering (NIS) experiments [8]. In fact the occurrence of the metal–nonmetal transition already suggests that the interatomic forces are subject to drastic changes, and consequently the behaviour of the total dynamic structure factor $S(Q, \omega)$ should be influenced by this. Localization of conduction electrons at ions (ionic bonding) or at bonds (covalent bonding) could lead to a shortening and a strengthening of the bonds which should be reflected in

0953-8984/97/5011035+09$19.50  

the position of the principal peak of $S(Q)$ and a frequency increase in $S(Q, \omega)$. Effects of this kind have in fact been observed in mixtures of pure liquid alkali metals with molten salts (with the same metallic component in the salt) in which the influence from ionic bonding is already observed at a salt addition of only 20 at.% to the pure liquid alkali metal, i.e. a concentration of only 10% of the chalcogenite [9]. Most recently also the atomic dynamics of liquid NaSn, an alloy with a tendency to form covalent bonds, was investigated [10]. However, to our knowledge no studies have so far been done on the collective atomic dynamics of such alloys, which should be especially sensitive to the character of the interatomic bonds. For this reason we have now started an investigation of the *collective excitations* in alloys with a tendency of forming interatomic bonds which are no longer pure metallic in character but have covalent or ionic components [11]. As a first step we have chosen the alkali-Sb system.

Besides its interest from a scientific point of view, the Rb–Sb alloy is a very favourable compound for a NIS experiment, due to its high coherent scattering cross-section compared with the incoherent one and because of the absorption cross-section, which always remains a factor two or three smaller than the scattering cross-section.

The aim of this research program therefore, is to study the influence of the variation of the Sb concentration $x$ in liquid alkali$_{1-x}$Sb$_x$ alloys on the interatomic forces via the investigations of the collective excitations in these liquids. Here we report the result of the first investigation at a concentration of $x = 0.05$ at 920 K well above the melting temperature of 840 K.

## 2. Experiment and data treatment

The experiment was performed at the cold neutron time focusing time-of-flight (TOF) spectrometer IN6 at the High Flux Reactor of the Institut Laue-Langevin in Grenoble. The $Rb_{95}Sb_5$ sample was kept in a thin walled (0.2 mm) vacuum tight (electron welded) niobium container and was heated in a vacuum of $10^{-5}$ Torr by the radiation from a thin vanadium-heating cylinder, which again was surrounded by several 0.05 mm thick concentric Nb heat shields. The thin walled Nb-container leads to a very good signal-to-noise ratio of our data. However, particularly at low momentum value transfers $\hbar Q$, the heating element and the heat shields contributed to the measured background near-zero energy transfer $\hbar\omega = 0$ and a special correction for those $Q$-values was necessary to remove the small sharp elastic peak which they added to the measured spectra. The region $-0.5 \leqslant \hbar\omega \leqslant 0.5$ (meV) was therefore excluded from the fits of the models to the data for $Q \leqslant 10.5$ nm$^{-1}$.

The incident energy was 4.75 meV; thus the TOF spectra could be measured up to 3.8 meV in neutron energy loss and to large negative energy transfers $\hbar\omega$ on the neutron energy gain side at scattering angles between 11 and 113 degrees, which were continuously covered with three rows of $^3$He detectors.

In order to extract $S(Q, \omega)$ from the experimental TOF spectra, a number of corrections have to be made. The raw data were corrected for the measured background (empty container run at 920 K), which is caused by the neutrons scattered from the surroundings of the sample (sample holder, furnace, vacuum chamber, etc) and by electronic noise. In this correction we took the difference in absorption of the filled and empty container into account. These intensities, due to the sample alone, were then corrected for the energy and scattering angle-dependent self-absorption of the sample and for the energy-dependent efficiency of each detector. Finally they were normalized to the solid angle (defined by the detector area corresponding to each spectrum and the TOF distance of 2483 mm), to the number of scattering units in the beam calculated from the known density of 1.75 g cm$^{-3}$ of the

sample at 920 K and to the incident neutron flux determined by the scattering cross-section of 5.1 barn of the vanadium sample, which we used in the vanadium calibration run and which had the same geometry as the sample. The FWHM of the peak of the elastically scattered neutrons (at $\hbar\omega = 0$) in the vanadium calibration spectra was 0.175 meV.

In order to correct the data for multiply scattered neutrons, a simulation of the experiment using the Monte Carlo program MSCAT [12] was made in which the histories of 20 000 neutrons were followed in each simulation run.

The sample scattering was described by the dynamic structure factor obtained from the Lovesey model. As the container walls were too thin to contribute appreciably to the multiple scattering of neutrons this was omitted in the simulation. The simulation was performed in a region where $S(Q, \omega)$ for the alloy was not zero, i.e. between $-30$ and 4 meV. Thus only this region has been analysed. We did not deconvolute the complicated resolution function of the time-focusing spectrometer, which increases rapidly with neutron energy gain transfers, but we have taken into account this finite resolution in the fit of the models to the experimental data, taking a mean value for the resolution in the energy region, where the collective excitations are found in the energy gain spectra, of 1 meV. No interpolation was done on the energy scale but time channels were summed up to give a nearly equidistant energy scale at smaller neutron energy gain and at energy loss transfers. The final $S(Q, \omega)$ values were interpolated by cubic splines in order to determine $S(Q = \text{constant}, \omega)$ under the assumption of an equal flight path from the sample to every detector.

## 3. Experimental results and discussion

In our experiment we measure the total dynamic structure factor which is the weighted sum of the partial dynamic structure factors; it is therefore necessary to state what are the partial contributions that are most important for our spectra.

In a binary alloy of component $A$ and $B$, the total dynamic structure factor $S(Q, \omega)$ can be expressed, in the Faber–Ziman representation [13] as

$$\sigma_{coh}^{sc} S(Q, \omega) = 4\pi(c_A b_A^2 S_{AA}(Q, \omega) + c_B b_B^2 S_{BB}(Q, \omega) + 2\sqrt{c_A c_B} b_A b_B S_{AB}(Q, \omega)) \qquad (1)$$

where $\sigma_{coh}^{sc} = 4\pi(c_A b_A^2 + c_B b_B^2)$ is the effective coherent scattering cross-section of the sample, $c_A$, $c_B$, $b_A$ and $b_B$ are respectively the concentration and the coherent neutron scattering lengths of the components $A$ and $B$, and $S_{ij}(Q, \omega)$ are the partial dynamic structure factors. From a single experiment we cannot determine the three partial contributions for which we would need three different experiments. In our case the contribution from the Rb correlations dominates as can be seen in table 1, even though the cross term is significant also.

**Table 1.** Weighting factors for the three partial dynamic structure factors in the Faber–Ziman and the Bathia–Thornton representation for $Rb_{95}Sb_5$.

| Faber–Ziman | | | Bathia–Thornton | | |
|---|---|---|---|---|---|
| $S_{AA}$ | $S_{BB}$ | $S_{AB}$ | $S_{NN}$ | $S_{CC}$ | $S_{NC}$ |
| 47.75 | 1.55 | 17.21 | 49.2 | 2.31 | 21.32 |

An alternative description of the total structure of a binary alloy is given by the correlations between particle density ($N$) and concentration ($C$) fluctuations in terms of

the three partial Bhatia–Thornton dynamic structure factors [14] $S_{NN}(Q,\omega)$, $S_{CC}(Q,\omega)$ and $S_{NC}(Q,\omega)$

$$\sigma_{coh}^{sc}S(Q,\omega) = \langle b\rangle^2 S_{NN}(Q,\omega) + (b_A - b_B)^2 S_{CC}(Q,\omega) + 2\langle b\rangle(b_A - b_B)S_{NC}(Q,\omega) \qquad (2)$$

where $\langle b\rangle = c_A b_A + c_B b_B$, $S_{NN}(Q,\omega)$ describes the correlation between density fluctuations, $S_{CC}(Q,\omega)$ the correlation between the concentration fluctuations and $S_{NC}(Q,\omega)$ is the cross correlation term.

In table 1 the weighting factor for the three Bathia–Thornton partial structure factors are also reported. We can conclude that in our experiment the measured total dynamic structure factor is determined substantially by the density–density correlation fluctuation with a non-negligible contribution from the cross correlation, while the contribution from the concentration–concentration fluctuations are essentially negligible.

An exact theory for the dynamic structure factor $S(Q,\omega)$ exists only in two limiting cases: for $Q \to 0$ and $Q \to \infty$; the first is well described by the linearized hydrodynamic theory which predicts $S(Q,\omega)$ to be a sum of three Lorenztians (plus two s-shaped correction terms), the central (Rayleigh) line due to the entropy fluctuations and two propagating sound modes (the Brillouin doublet caused in liquids with not too high viscosity; only longitudinal excitations are excited in Brillouin scattering experiments). The second limit ($Q \to \infty$) is that of the ideal gas (single-particle motion only) and in this limit $S(Q,\omega)$ is described by a Gaussian profile [15].

The hydrodynamic theory is still applicable when the product of $Q$ with the mean free path of the atom $l$ is well below one (only in this case one is still near the hydrodynamic limit and it makes sense to speak of propagating sound modes). In our case, assuming for $l$ the Enskog mean free path $l_E$ (hard sphere model)

$$l_E = \frac{1}{n\pi\sigma^2 g(\sigma)\sqrt{2}} \qquad (3)$$

and taking for $s$ the value reported by Block *et al* [16] and for $g(s)$ the value by Winter *et al* [2] (both for pure rubidium) we obtained for $l_E \sim 1.6$ Å. This leads to a maximum value of $Q$ of the order $\sim 6$ nm$^{-1}$ at which the hydrodynamic theory should still be applied. In our case the lowest $Q$ value obtained is 10 nm$^{-1}$; thus only a generalized hydrodynamic model could be expected to be applicable to our data. Between the two limits mentioned above, various models have been developed such as the generalized hydrodynamic description [17] or modified kinetic theories [18]. Here we apply a simple meanfield theory to the data in choosing the model of Lovesey [19], that gives a simple expression for $S(Q,\omega)$ as an approximate solution of Mori's generalized Langevin equation for the density correlation function

$$S(Q,\omega) = \frac{Q^2}{\pi\beta M}\frac{\tau(Q)(\omega_l^2(Q) - \omega_0^2(Q))}{[\omega\tau(Q)(\omega^2 - \omega_l^2(Q))]^2 + (\omega^2 - \omega_0^2(Q))^2}. \qquad (4)$$

In equation (4) $M$ is the mass of the atom, $b = 1/k_B T$, with $k_B$ the Boltzmann constant and $T$ the temperature. $\omega_0^2 = \langle\omega^2\rangle/\langle\omega''\rangle$ represent the ratio of the second to the zeroth frequency moment of the dynamic structure factor

$$\langle\omega^n\rangle = \int \omega^n S(Q = \text{constant},\omega)\,\mathrm{d}\omega \qquad (5)$$

$\omega_l^2 = \langle\omega^4\rangle/\langle\omega^2\rangle$ is the ratio of the fourth to the second moment of $S(Q,\omega)$ and $t$ is a relaxation time of the viscosity.

In the classical limit, the recoil effects being omitted, the following relations hold for the isothermal dispersion

$$\omega_0^2(Q) = \frac{k_B T}{M}\frac{Q^2}{S(Q)} \tag{6}$$

and for the adiabatic dispersion

$$\omega_l^2(Q) = 3\langle\omega^2\rangle + \frac{n}{M}\int g(r)(1-\cos(Qz))\frac{\partial^2 V(r)}{\partial z^2}\,\mathrm{d}^3 r \tag{7}$$

where $n$ is the number density, $V(r)$ is the pair potential and $g(r)$ the radial correlation function.

The approximation we make in using this model, which was originally derived for a monatomic liquid, is not too severe as we have shown before that the dominant part of the observed scattering stems from Rb.

Figure 1 shows a three-dimensional representation of the experimental dynamic structure factor of $Rb_{95}Sb_5$ at 920 K.

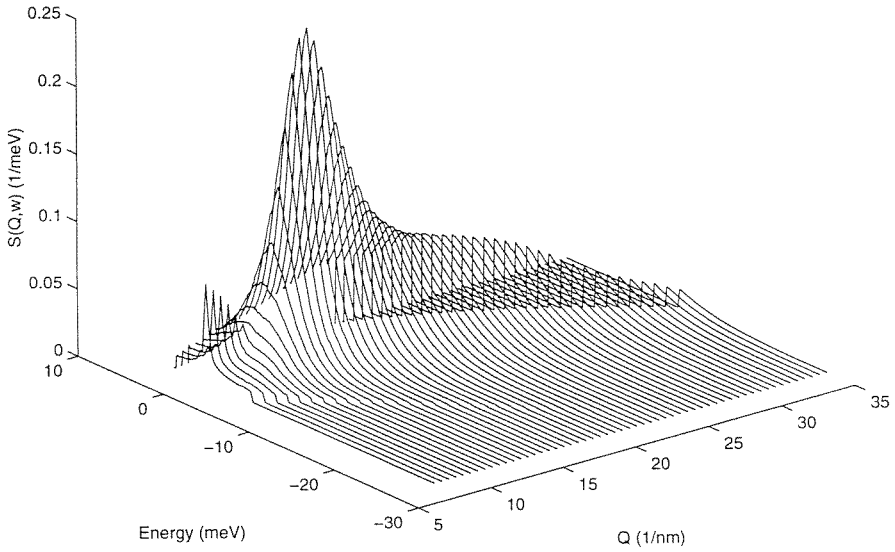


**Figure 1.** The total dynamic structure factor of $Rb_{95}Sb_5$ determined at 920 K and at $Q$-values between 8 and 35 $nm^{-1}$ and energies between $-29$ and 4 meV. The central peaks at smallest $Q$-values may be due to an incomplete background correction.

Integrating $S(Q,\omega)$ at $Q =$ constant over $\omega$, (see equation (5)), we obtain the zeroth frequency moment, the static structure factor $S(Q)$, that is reported in figure 2 together with three $S(Q)$ curves for pure liquid rubidium measured at 773, 1073 and 1373 K respectively [20]. From this two important pieces of information can be obtained. The position of the principal maximum of $S(Q)$ at $Q_p$ of pure rubidium decreases continuously with temperature (see figure 2) and for $T = 920$ K $Q_p$ is expected to be 15.0 $nm^{-1}$ for pure Rb where we cannot give an error bar nor the pressure for these unpublished data [20]. The $Q_p$ value for $Rb_{95}Sb_5$ at 920 K however is $15.4 \pm 0.25$ $nm^{-1}$. This means that the mean bond length in $Rb_{95}Sb_5$ has become shorter by about 2% than that in pure liquid Rb at the same temperature but higher pressure by adding 5% of Sb. We arrive at the same conclusion if we use the

quantitative information contained in the publication of earlier data on the static structure factor of Rb near the vapour pressure line [21]. Here the decrease of $Q_P$ is given in table 1 [21] without indication of error bars. A polynomial fit of the first three values of this table results in a mean slope of about 7.6 $10^{-4}$ $nm^{-1}$ $K^{-1}$. The corresponding linear change in the position $r_P$ of the main maximum of the radial correlation function $g(r)$ (given in their figure 2) is approximately 1.05 $10^{-5}$ nm $K^{-1}$. Combined with their measured value of $Q_P$ (900 K) = 14.7 $nm^{-1}$ (near vapour pressure) and $r_P \approx 0.5$ nm this leads to a change in $r_P$ of 2% in our case compared with Rb near its vapour pressure at the same temperature. The second observation concerns the low $S(Q)$ values for $Rb_{95}Sb_5$ compared to pure Rb. This fact, already observed by Lamparter *et al* in Cs–Sb alloys [6], could be caused in our case by the contribution from the density-concentration cross term to the total structure factor. The low value is not due to an incomplete integration of $S(Q, \omega)$, as in the $Q$-region near $Q_P$ its dominant contribution stems from a relatively narrow quasielastic energy region near $\omega = 0$.

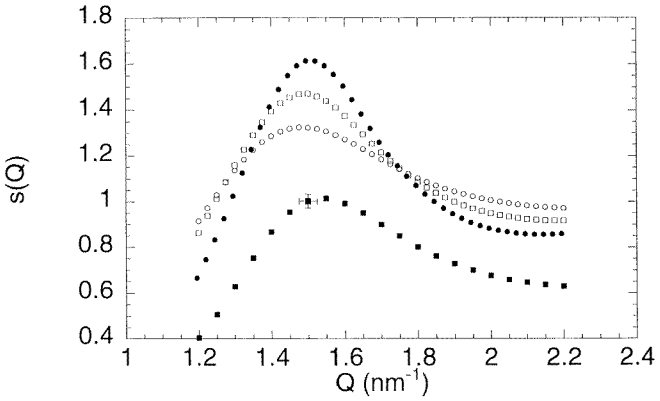


**Figure 2.** The static structure factor for $Rb_{95}Sb_5$ at 920 K (full squares) is compared with the static structure factor for pure rubidium at 773 K (full circles), 1073 (empty squares) and 1373 (empty circles) [20]. The shift of the maximum to smaller $Q$-values is obvious.

We have fitted these $S(Q, \omega)$ data at $Q$ = constant with Lovesey's model, leaving $\omega_0(Q)$, $\omega_l(Q)$ and $\tau(Q)$ as free parameters. The fits are very good for $11.0 \leqslant Q \leqslant 20.0$ $nm^{-1}$, and acceptable for $Q < 11.0$ $nm^{-1}$ and $Q > 20.0$ $nm^{-1}$. An example of the fit for $Q = 16.5$ $nm^{-1}$ is given in figure 3.

In figure 4 the three parameters $\omega_0(Q)$, $\omega_l(Q)$ and $1/\tau(Q)$ obtained from the fits are reported as a function of $Q$. For the adiabatic and isothermal dispersion we could determine the branch with negative and with positive slope with the minimum between 14.5 and 15.0 $nm^{-1}$, next to $Q_p$. Comparing our result with a preliminary fit of $S(Q, \omega)$ of pure Rb measured at 393, 593 and 773 K [23] we again observe a shift of the minimum of the adiabatic and the isothermal dispersion to a higher $Q$ value than expected for pure rubidium at 920 K (extrapolated from the three pure Rb curves) and most likely also higher energy values for both of the two $Rb_{95}Sb_5$ dispersion curves than expected for pure rubidium at 920 K, although this conclusion is within the error bars of the dispersions for $Rb_{95}Sb_5$ and for pure Rb extrapolated at 920 K. In order to achieve a more quantitative comparison with previous work on pure Rb [22] we determined also the dispersion $\omega_m(Q)$ from the maxima in the longitudinal current–current correlation function $J_l(Q, \omega) = \omega^2 S(Q, \omega)/Q^2$. Comparing the dispersion $\omega_m(Q)$ for our sample with that obtained by Chieux *et al* [22] for

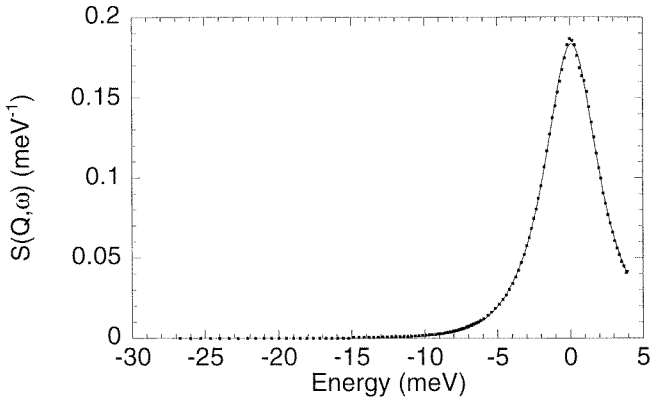


**Figure 3.** Fit of the Lovesey model to the dynamic structure factor of $Rb_{95}Sb_5$ measured at 920 K and at $Q = 16.5$ nm$^{-1}$.

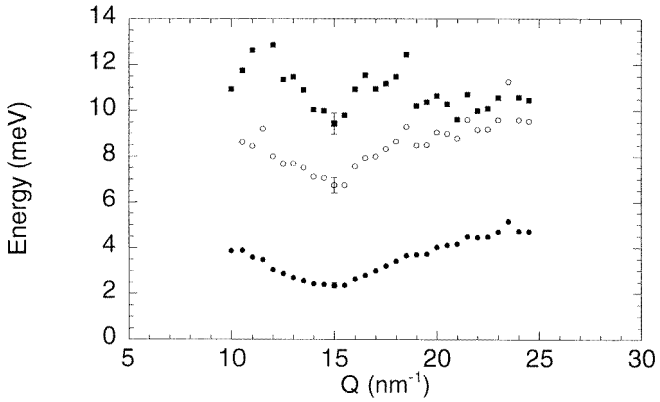


**Figure 4.** Isothermal $\omega_0$ (full circles) and adiabatic $\omega_l$ (empty circles) dispersions together with the inverse of the relaxation time $1/\tau$ (full squares) obtained from the fit of the Lovesey model as a function of $Q$ for $Rb_{95}Sb_5$ at 920 K.

pure rubidium at 393, 593 and 776 K, (see figure 5) one realizes that the dispersion curve for $Rb_{95}Sb_5$ is at considerably higher energies than expected for liquid Rb at 920 K. The increase of the $\omega_m(Q)$ of $Rb_{95}Sb_5$ with respect to those of rubidium by about 20% in the mean indicates a strengthening of the bonds in $Rb_{95}Sb_5$ by the addition of Sb to pure Rb.

For a further comparison of our data with previous results presented in the literature [22], we fitted the $S(Q = \text{const}, \omega)$ data also with the generalized kinetic theory retaining only three of the infinitely many Lorentians as one does in the hydrodynamic limit. However, as we allowed the parameters to be functions of the momentum transfer this limitation represents only a weak approximation even though the hydrodynamic limit does not apply to our experimental condition. The conclusion drawn from the comparison of the dispersion obtained from the fits of the kinetic theory to our data and to pure Rb [22] is the same as for the dispersion obtained from the current–current correlation function, i.e. in our case the dispersion has higher energies compared with those expected for pure rubidium at 920 K. In figure 6 we show a fit with three Lorentians at $Q = 10.5$ nm$^{-1}$ together with the width

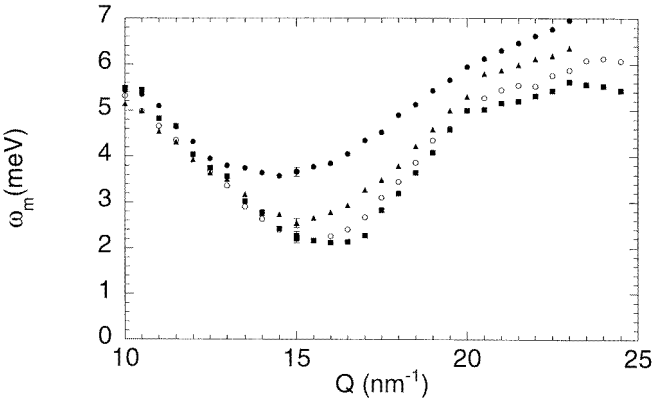


**Figure 5.** The maxima $\omega_m(Q)$ of the longitudinal current–current correlation function $J_l(Q,\omega)$ for $Rb_{95}Sb_5$ at 920 K (full circles) compared with the $\omega_m(Q)$ values for pure rubidium at 393 K (full squares), 593 K (empty circles) and 776 K (full triangles) [22]. The shift to higher energies and smaller $Q$-values is well demonstrated.

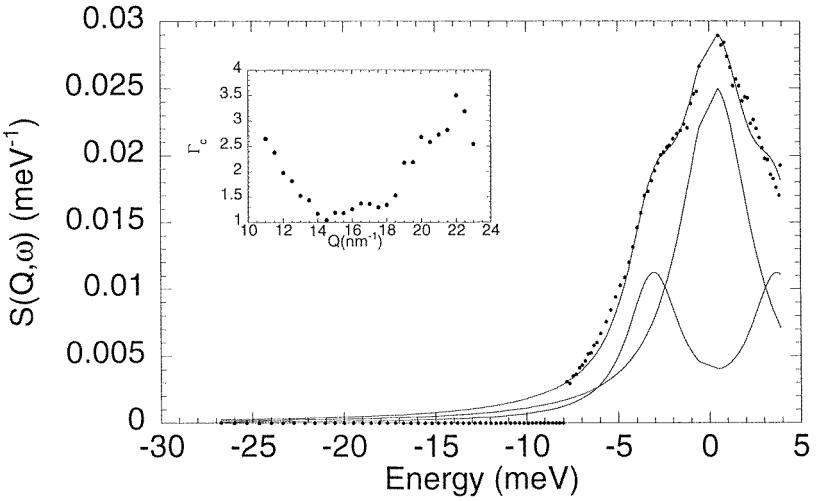


**Figure 6.** Fit of the kinetic model (three Lorentians) to the dynamic structure factor for $Rb_{95}Sb_5$ at 920 K and at $Q = 10.5$ nm$^{-1}$. The inset shows the width of the central line $\Gamma_c$ as function of $Q$.

of the central line as a function of $Q$, in which one observes a quite pronounced de Gennes narrowing [24].

## 4. Conclusions

From the analysis of the total static structure factor and of the dispersion curves obtained from the total dynamic structure factor we conclude that 5% of Sb in liquid Rb is sufficient to cause an observable shortening and strengthening of the bonds compared to the values extrapolated for pure liquid rubidium at the temperature of the experiment even though the

general character of the alloy is still metallic at this small concentration. The investigation up to now has concentrated on one Sb-concentration and it would therefore be premature to conclude a general trend from these first investigations. From the NMR-investigations done by Dupree *et al* [25] in a different region of energy and time-scale we presently expect to see the influence of electron localization first on predominantly ionic bonds near $Rb_3Sb$ and then at more covalent bonding at RbSb when increasing the Sb concentration up to the metal–nonmetal transition in further experiments.

## Acknowledgments

It is a pleasure to thank H Teichmann for part of the preparation of the sample, A J Dianoux and S Jenkins for their help at the start up of the experiment and P Andant for his assistance at the furnace. This work was performed under CE-grant No ERBCHBGCT940700.

## References

[1] Winter R, Pilgrim W C and Hensel F 1994 *J. Phys.: Condens. Matter* **6** A245
[2] Winter R, Pilgrim C, Hensel F, Morkel C and Gläser W 1993 *J. Non-Cryst. Solids* **156–158** 9
[3] Brinkmann R, Paulick C A, Elwenspoek M, Von Hartrott M, Kiehl M, Maxim P and Quitmann D 1985 *Phys. Lett.* **111A** 435
[4] Redslob H, Steinleitner G and Freyland W 1982 *Z. Naturforsch.* **27a** 587
[5] Ott K, Dürrwächter M, Haghani M A and Quitmann D 1992 *J. Non-Cryst. Solids* **142** 278
[6] Lamparter P, Martin W, Steeb S and Freyland W 1983 *Z. Naturforsch.* **38a** 329
[7] Bernard J and Freyland W 1996 *J. Non-Cryst. Solids* **205–207** 62
[8] For a recent review see J-B Suck 1993 *Int. J. Mod. Phys.* **7** 3003
[9] Chieux P, Dupuy-Philon J, Jal J-F, Morkel C and Suck J-B 1994 *J. Phys.: Condens. Matter* **6** A235
[10] Saboungi M-L, Johnson G K and Price D L 1994 *Proc. NATO ASI Stat. Dyn. Alloy Phase Transform.* ed P E A Turchi and A Gonis (New York: Plenum)
[11] Hafner J 1996 private communication
[12] Copley J, Verkerk P, Van Well A A and Fredrikze H 1986 *Comp. Phys. Comm.* **40** 337
[13] Faber T E and Ziman J M 1965 *Phil. Mag.* **11** 153
[14] Bathia A B and Thornton D E 1970 *Phys. Rev.* B **2** 3004
[15] Copley J R D and Lovesey S W 1975 *Rep. Prog. Phys.* **38** 461
[16] Block R, Suck J-B, Freyland W, Hensel F and Gläser W 1977 *(Inst. Phys. Conf. Ser. 30)* ed R Evans and D A Greenwood (Bristol: Institute of Physics) p 126
[17] Boon J P and Yip S 1980 *Molecular Hydrodynamics* (New York: McGraw-Hill)
[18] de Schepper M and Cohen E G D 1980 *Phys. Rev.* A **22** 287
[19] Lovesey S W 1971 *J. Phys. C: Solid State Phys.* **4** 3057
[20] Winter R 1996 private communication
[21] Franz G, Freyland W, Gläser W, Hensel F and Schneider E 1980 *J. Physique* **41** C8–194
[22] Chieux P, Dupuy-Philon J, Jal J-F and Suck J-B 1996 *J. Non-Cryst. Solids* **205–207** 370
[23] Suck J-B *et al* 1996 unpublished results
[24] deGennes P G 1959 *Physica* **25** 825
[25] Dupree R, Kirby D J and Freyland F 1982 *Phil. Mag.* B **46** 595